ADVANCED FUNCTIONAL MATERIALS
www.afm-journal.de

A Colorimetric Hydrocarbon Sensor Employing a Swelling-Induced Mechanochromic Polydiacetylene

*Dong-Hoon Park, Jaesung Hong, In Sung Park, Chan Woo Lee, and Jong-Man Kim**

Exceptional challenges have confronted the rational design of colorimetric sensors for saturated aliphatic hydrocarbons (SAHCs). The main reasons for this difficulty are the extremely nonpolar nature of these targets and their lack of functional groups that can interact with probes. By taking advantage of a mechanochromic conjugated polydiacetylene (PDA) and the hydrocarbon-induced swelling properties of polydimethylsiloxane (PDMS), a sensor film that enables simple, colorimetric differentiation between a variety of C5 to C14 aliphatic hydrocarbons is fabricated. The unprecedented PDA–PDMS composite sensor undergoes a blue-to-red colorimetric transition on a time-scale that is dependent on the chain length of the hydrocarbon target. In addition, the development of the red color is directly proportional to the swelling ratio of the film. This straightforward approach enables naked-eye differentiation between n-pentane and n-heptane. The versatility of the sensor system is demonstrated by using it for the colorimetric determination of kerosene in adulterated diesel oil. Finally, the observation that a PDA microcrystal in the film undergoes significant expansion and tearing in concert with a blue-to-red colorimetric transition during the swelling process provides direct evidence for the mechanism for the mechanochromic behavior of the PDA.

1. Introduction

Recently, polymeric materials that undergo visible (400–800 nm) absorption and emission spectral changes in response to external mechanical stimuli have attracted significant attention owing to their applications in visible strain sensor and deformation detector systems, and in anti-counterfeiting and optical memory devices.[1–4] For these purposes, a variety of mechanochromic functional dyes have been incorporated into polymer matrices either noncovalently[5–7] as supramolecular aggregates or covalently[2,4] in the form appendages to polymer chains. Colorimetric transitions of mechanochromic polymer systems of this type usually occur when functional dyes in the polymer matrix undergo either changes in their stacking interactions or chemical transformations upon mechanical stimulation. In addition, periodically structured polymeric photonic gels have also gained much attention for their mechanochromic properties.[8,9]

Polydiacetylenes (PDAs)[10–22] are structurally very unique conjugated polymers. These polymers that possess alternating ene-yne conjugated structures are prepared from self-assembled supramolecular diacetylene (DA) monomers. Owing to the existence of extensively delocalized π-electron networks and conformational restrictions present along the main chain, PDAs have unique optical properties. In particular, PDAs undergo distinct color changes (typically blue-to-red) when their arrayed p-orbitals are distorted under the influence of environmental perturbations (eg., heat, solvent, current, magnetic field, strain force, ions, ligand-receptor interactions).[23–47]

Mechanochromic properties of PDAs have also been probed.[48–50] For example, a blue-to-red (or yellow) color transition is observed to take place when a PDA-polyurethane copolymer is subjected to tensile elongation.[48] This finding indicates that if a proper amount of mechanical stretching energy is delivered to PDA chains, disruption of the p-orbital array occurs to promote a colorimetric transition.

In the study described below, special attention has been given to the polydimethylsiloxane (PDMS) elastomer, a low cost, flexible and optically transparent polymer that has been reported to undergo significant increases in volume when exposed to saturated aliphatic hydrocarbons (SAHCs).[51] Moreover, the swelling ratios of PDMS promoted by linear alkanes are inversely proportional to the number of methylene units in the carbon chain (eg., 1.44 in pentane, 1.34 in heptane). The combined observations that PDA mechanochromism takes place during tensile elongation and PDMS swelling occurs in the presence of hydrocarbons have led to the proposal that placement of a PDA-incorporated PDMS film in a liquid hydrocarbon should lead to swelling of the matrix causing mechanical stress that will be transferred to an embedded PDA supramolecule. If the energy transferred to the PDA in this manner is large enough to disrupt the ordered structure of the PDA chains, a colorimetric transition of the film will take place. Finally, the different swelling ratios of PDMS in the PDA-embedded PDMS film upon exposure to different SAHCs

D.-H. Park, J. Hong, I. S. Park, Prof. J.-M. Kim
Department of Chemical Engineering
Hanyang University
222, Wangsimni-ro, Seongdong-gu, Seoul 133–791, Korea
E-mail: jmk@hanyang.ac.kr
Prof. C. W. Lee, Prof. J.-M. Kim
Institute of Nano Science and Technology(INST)
Hanyang University
222, Wangsimni-ro, Seongdong-gu, Seoul 133–791, Korea
DOI: 10.1002/adfm.201400779

should serve as the foundation for a novel sensing system that can be used to detect and differentiate hydrocarbons.

If correct, the above proposal will address one of the most challenging issues in the chemical and material sciences revolving about the development of sensor systems that undergo color changes upon interaction with SAHCs. Until now, the nonpolar and functional group (hydrogen/ionic bonding or electron donor/acceptor moieties) deficient nature of SAHCs have served as large barriers for the rational design of efficient colorimetric SAHC sensors. Although hydrocarbon sensors, which are based on fluorescent dye displacement,[52] polycyclic aromatic hydrocarbons,[53] inorganic nanowires,[54] photonic crystals,[55] and viscosity sensitive fluorescent polymers,[56] have been described, these methods either require expensive instrumentation to read output signals and/or suffer from preparation/operational complexity.

As part of our continuing efforts focusing on the development of PDA-based solvatochromic sensors,[57–59] we have employed the reasoning given above to design an unprecedented colorimetric hydrocarbon sensor system that synergically employs the effects of PDA mechanochromism and PDMS swelling. The new solvatochromic sensor system possesses many important features. Firstly, the colorimetric signal, generated upon exposure of the sensor to SAHCs, is easily recognized by using the naked eye. Secondly, the sensor can be employed to visually differentiate structurally similar SAHCs (eg., n-pentane and n-heptane). Thirdly, the sensor system is readily fabricated from a commercial DA monomer and PDMS precursor by using a simple, sequential mixing-irradiation-curing procedure. Fourthly, in a practical sense, the sensor can be employed to determine the presence of kerosene in adulterated diesel oil. In addition, this effort has demonstrated for the first time that a PDA microcrystal undergoes tearing from edge sides during the PDMS swelling process and that this phenomenon simultaneously promotes a blue-to-red color change. Finally, the strategy developed in this investigation has the potential of serving as the foundation for the design of a variety of tailor made colorimetric hydrocarbon sensors that are comprised of properly selected mechanochromic dyes and PDMS elastomers.

2. Results and Discussion

2.1. Fabrication of the PDA-embedded PDMS Film

In an effort designed to investigate the feasibility of PDA-PDMS composite based SAHC sensor systems, a PDMS film containing PDA supramolecules was fabricated employing a simple mixing-irradiation-curing method (**Figure 1**). Specifically, a chloroform solution (0.2 mL), containing commercially available 10,12-pentacosadiynoic acid (PCDA) (Figure 1a), was injected into the PDMS elastomer base (1.0 g). After chloroform was removed in vacuo, the mixture was irradiated with a 254 nm UV lamp (1 mWcm^{-2}) for 1 min while stirring to induce photopolymerization of the PCDA molecules. Formation of blue color upon UV irradiation is indicative of the presence of PDA supramolecules in the material. Following addition of a curing agent (10:1 wt ratio), the resulting blue colored, viscous mixture was poured into a Petri dish, degassed *in vacuo*, and cured at room temperature for 2 days. This process generated a flexible, transparent, ca. 600 μm thick, PDA-incorporated PDMS film (see Figure 1b).

Visible absorption spectroscopic monitoring of the process confirmed that PDAs are present in the PDMS matrix (Supporting Information, Figure S1). An optical microscopic image of a PDA-PDMS composite film clearly demonstrates

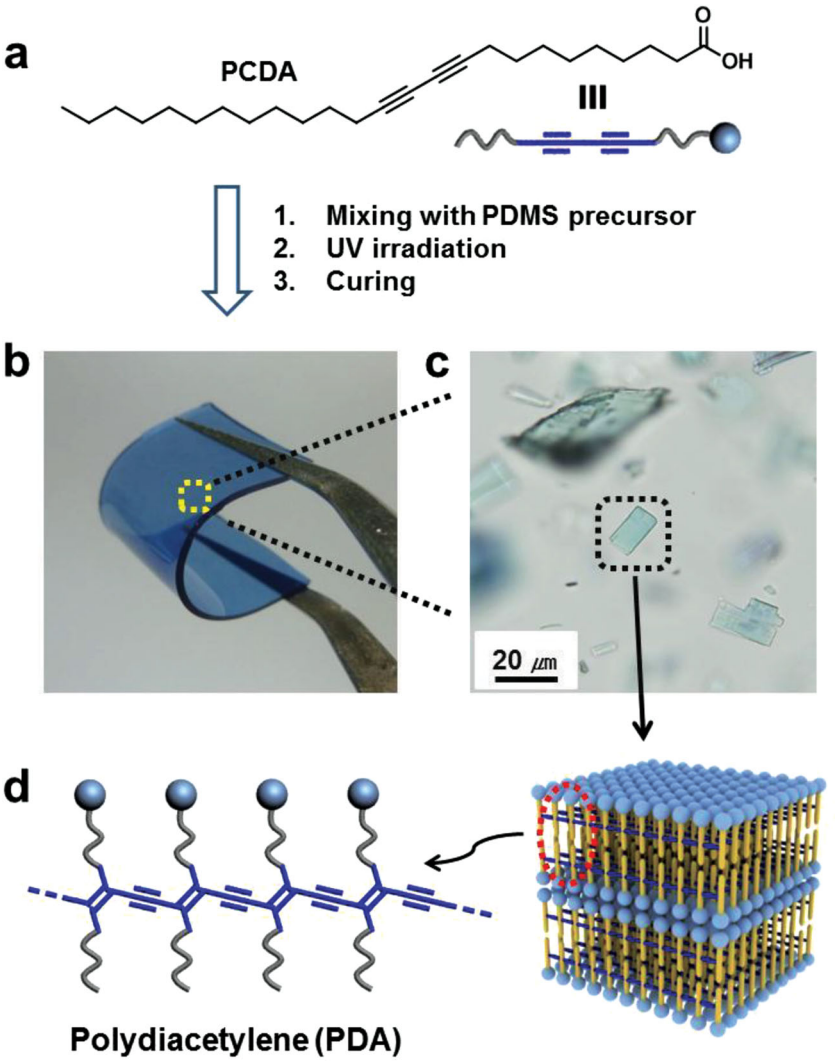

Figure 1. (a) Structure of PCDA. (b) Photograph of a typical PDA-embedded PDMS film. (c) Optical microscopic image of the PDA-embedded PDMS film (d) Schematic of PDA supramolecules.

that the PDA particles are well-dispersed in the PDMS film (Figure 1c), as represented schematically by layered supramolecular PDAs in Figure 1d. It should be noted that fabrication of stable blue-colored PDA-embedded films is difficult when other substances such as polystyrene (PS), poly(methyl methacrylate) (PMMA), poly(ethylene oxide) (PEO) and poly(vinyl chloride) (PVC) are employed as matrix polymers (Supporting Information, Figure S2). This observation demonstrates the meritorious feature of the PDMS matrix.

2.2. Colorimetric Response to Hydrocarbons

A very surprising result arose from initial studies in which responses of the PDA-embedded PDMS film to hydrocarbons were probed. Upon being placed in n-pentane, the size of the sensor film immediately started to grow in concert with the occurrence of a gradual color change from blue-to-purple-to-red (**Figure 2**a). The red color reached a maximum intensity within 5 min of the start of the incubation process (Figure 2b). Incubation of the PDA-PDMS sensor film in a pentane for 10 min brought about a 320% increase in its volume (Figure 2c, middle) and the film returned to its original volume when it was removed from pentane and allowed to stand (Figure 2c, right) (Supporting Information, Movie S1).

Equally interesting were the results of studies, which showed that the PDA-PDMS sensor film responds differently to different SAHCs. For instance, incubation of the sensor film in pentane (C5), heptane (C7) and nonane (C9) for 5 min promotes significantly different levels of color change (Figure 2d, inset). The strips after drying display pale red (C5), purple (C7) and purple blue (C9) colors, respectively. The different colorimetric responses indicate that pentane is superior to heptane and nonane in its ability to disrupt the supramolecular order of the PDA chains. It should be noted as an aside that, although incubation of the PDA powder in hydrocarbons results in some colorimetric changes, they are not sufficiently large to enable visual differentiation of the SAHCs (Supporting Information, Figure S3).

Visible absorption spectroscopy was used to confirm the colorimetric changes occurring in the PDA-PDMS sensor films (Figure 2d). A significant decrease in the intensity of the absorption band at 641 nm, associated with the blue phase of the PDA, along with a simultaneous increase in the intensity of the band at 545 nm take place when the film is exposed to pentane. In addition, the magnitude of the decrease in the intensity of the 641 nm band decreases with solvent in the order: pentane > heptane > nonane.

Because the colorimetric response is proposed to be associated with volume changes, swelling ratios of the PDA-PDMS sensor film in various alkanes were determined. The swelling ratio for incubation of a 600 μm thick PDMS film in linear alkanes for 10 min was found to decrease consistently in the following manner: C5 (1.468), C7 (1.326), C9 (1.241), C11 (1.167), C13 (1.120). In addition, the degree of increase in red intensity of the PDA-embedded PDMS film following incubation for 10 min in these SAHC was found to decrease as the number of carbons in the alkane increases (**Figure 3**a). These observations, visualized in the movie clip provided in Supporting Information (Movie S2), clearly show that the rate of swelling and color change of the PDA-PDMS sensor film upon exposure to linear alkanes is strongly dependent on the length of the hydrocarbon chain with larger rates being associated with shorter alkyl chains.

In the next phase of the investigation, we determined times required for the sensor strip to reach a fixed red intensity (RI) value following exposure to various hydrocarbon solvents. As expected based on observations described above, the times required for the sensor strip to reach 75% RI increase as the chain length of the linear alkane increases (Figure 3b). Linear alkanes of higher carbon numbers than decane require over a 30 min incubation time to reach the 75% RI value. The data show this sensor enables differentiation between two SAHCs differing by only one carbon, a remarkable finding in light of

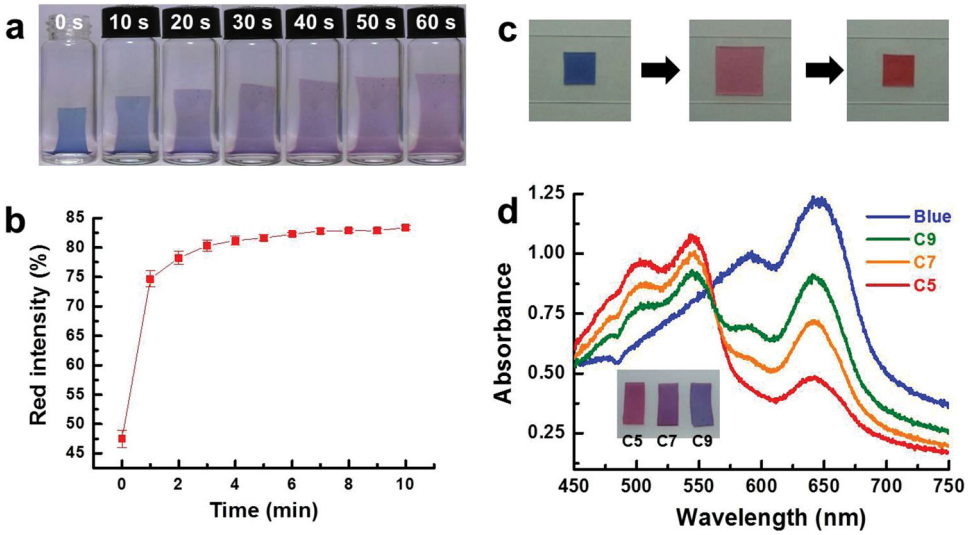

Figure 2. (a) Images showing the time dependent colorimetric response and swelling behavior of a PDA-PDMS film in a pentane solvent. (b) Plots of the red intensity of a PDA-PDMS film in pentane as a function of time. (c) Images showing the swelling and shrinking behavior of a PDA-PDMS composite film upon exposure to pentane. (d) Visible absorption spectra of PDA-PDMS films obtained after incubation in designated solvents for 5 min. The inset shows photographs of dried PDA-PDMS films after 5 min incubation in pentane (left), heptane (middle), and nonane (right).

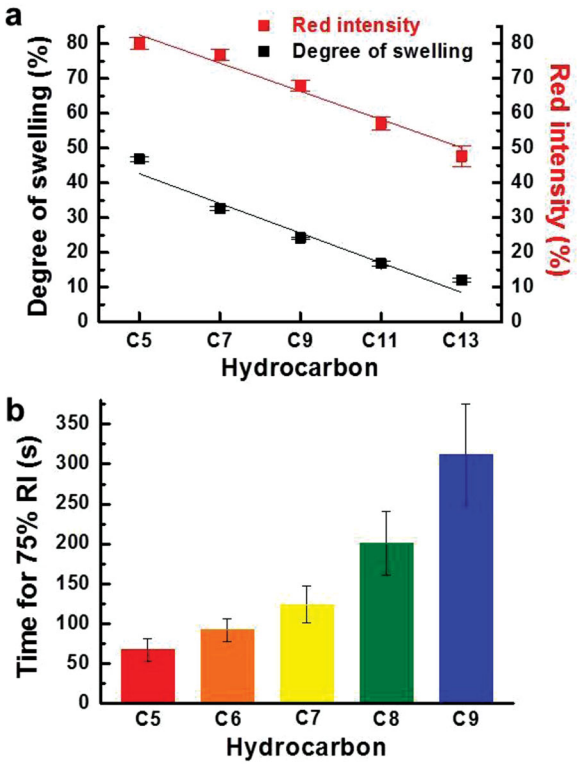

Figure 3. (a) Plots of red intensity and degrees of swelling of a PDA-embedded PDMS film after 10 min incubation in linear alkanes possessing different chain lengths, showing that red intensity development is proportional to the swelling ratio of the polymer film. (b) Bar graph showing that the time required for the PDA-embedded PDMS film to reach to a 75% red intensity (RI) value increases as the alkane chain length increases.

previous difficulties encountered in designing colorimetric hydrocarbon sensors.

Another feature of the PDA-PDMS sensor is that colorimetric response of the sensor is dependent on the thickness of the film and the amount of PDA presents in the PDMS matrix (Supporting Information, Figure S4). Thus, the degree of increase in red intensity developed from a 3 min incubation of a PDA-embedded PDMS film in heptane was observed to decrease as the film thickness increases (Supporting Information, Figure S4, a). In addition, the degree of increase in red intensity was found to be inversely proportional to the amount of the PDA supramolecules in the PDMS matrix (Supporting Information, Figure S4, b). Overall, the best performance was achieved with a sensor film of 600 μm thickness that was prepared from a mixture of 2.5 mg of PCDA and 1 g of PDMS base.

2.3. Practical Application

The number of cases in which fake and adulterated petroleum is sold has increased dramatically worldwide in recent times. For instance, John Hogg, one of the world's forerunners in marketing fuel markers, has estimated that the UK loses more than GBP 500 million each year as a result of automotive fuel tampering.[60] Especially problematic because of taxation concerns in many countries are illegally formulated diesel oils, which are generated by adding relatively cheap kerosene to more heavily taxed diesel fuel. Kerosene is typically used as a heating fuel for households in many countries and is sold at lower prices (for instance 1.4 US$ per liter, in Korea) than is diesel (1.8 US$ per liter). Since the compositions of kerosene and diesel are similar (ca. 80% identical), detection of adulterated diesel oil is difficult. In an attempt to prevent counterfeiting, commercial kerosene normally contains a small amount of an indicator (eg. phenolphthalein derivatives) so that adulterated diesel oil can be readily identified. The currently used indicators, however, can be easily removed from kerosene by filtration through active carbon.

Owing to these issues, a simple, relatively inexpensive, on-the-spot detection system that can be employed to identify adulterated diesel is in great demand. Because kerosene is composed of C6-C16 hydrocarbons while diesel oil contains hydrocarbons ranging up to C8-C21, we believed that the new PDA-PDMS composite film might be applicable for this purpose. Indeed, incubation of the sensor film in commercial kerosene and diesel was observed to promote visually distinguishable colorimetric responses (inset figure in **Figure 4**). Specifically, upon exposure to kerosene the PDA-embedded PDMS sensor film undergoes a blue to purple-red transition while no significant color change occurs when the film is immersed in diesel. In addition, the amount of kerosene added to diesel oil can be determined by simply measuring the RI value of the film after a 10 min incubation period (Figure 4). These observations suggest that a potentially useful on-the-spot sensing system to detect adulterated diesel would be composed of the PDA-embedded PDMS sensor film and a simple portable reflectometer.

2.4. Mechanistic Considerations

The swelling induced color change that the PDA-embedded PDMS film undergoes when exposed to SAHCs is mechanistically

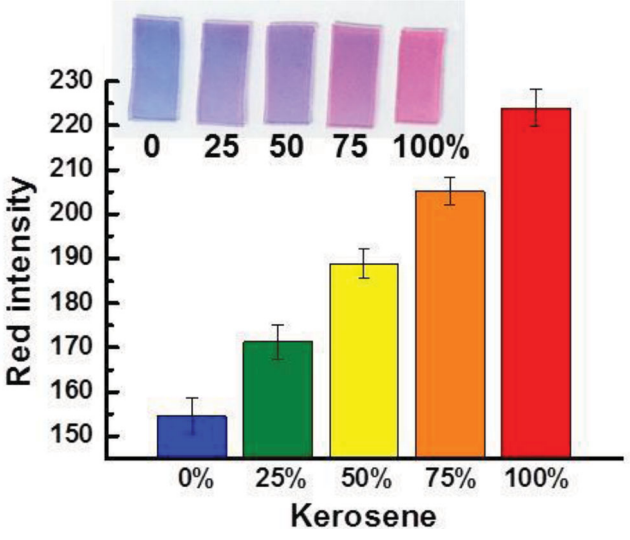

Figure 4. Bar graph showing the colorimetric response of the sensor film after 10 min exposure to various volume compositions of kerosene in diesel oil. The inset shows photographs of the corresponding films.

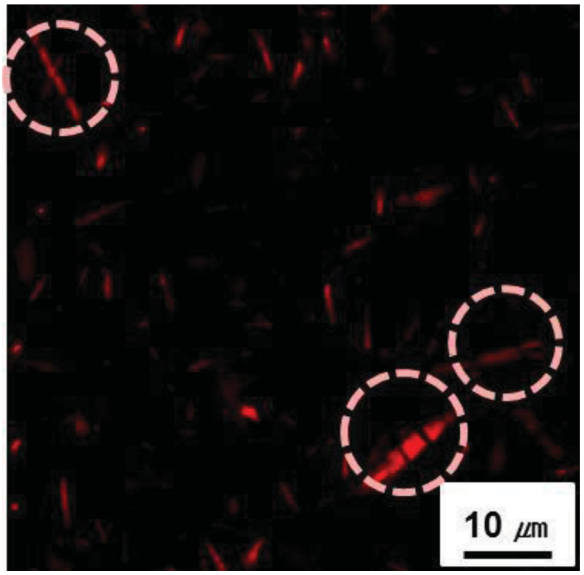

Figure 5. Confocal fluorescence microscopic image of a PDA-embedded PDMS film, obtained after incubation in pentane for 5 min.

intriguing. An interesting feature of this process was revealed in studies in which changes taking place in the PDA-embedded PDMS strip are monitored using a confocal fluorescence microscope. A pentane incubated, red-colored sensor film was observed to display segmented fluorescence emission from some but not all PDA crystals within the film (**Figure 5**, PDAs inside the circles). This phenomenon is not observed when the PDA-PDMS composite film undergoes the blue-to-red color transition upon heat treatment (Supporting Information, Figure S5). We initially thought that the segmented fluorescence emission originated from different, closely located PDA crystals. However, analysis of fluorescence images collected from diverse samples confirmed that emission arises from edges where PDA crystals had undergone rupture (Supporting Information, Figure S6).

Motivated by the results of the confocal fluorescence microscopic studies, our attention next focused on an effort to gather direct evidence for the role played by PDA crystal tearing during hydrocarbon induced film swelling. We envisioned that optical microscope analysis of a PDA microcrystal located close to the surface of PDMS film might provide important information about the mechanochromic event. Indeed, this approach showed that a blue-colored PDA microcrystal near the surface of the PDMS film exposed to octane does indeed undergo a dramatic, time-dependent morphological change along with a simultaneous blue-to-red color transition (**Figure 6**a). Importantly, inspection of the microscope image reveals that initiation of tearing occurs from the weak edge side of the PDA crystal. Thus, these findings are fully consistent with the observed segmented fluorescence images (Figure 5) discussed above. In Figure 6b are shown schematic top views of the PDA crystal displayed in Figure 6a during the hydrocarbon promoted swelling process. Mechanical strain energy, transferred to PDA crystals as a consequence of film swelling, should have a major impact on edge sides where attractive forces between neighboring PDA chains are expected to be low. Thus, separation of the PDA chains should occur from the weak edge sides and eventually migrate to the middle part of the crystal. The increase in interchain distance caused by this change enables a certain degree of C-C single bond free rotation to occur in the polymer main chains, which leads to distortion of the arrayed p-orbitals and the consequent blue-to-red color transition (Figure 6c).

We found that simple mechanical stretching of the PDA-embedded PDMS film does not cause a noticeable color change. This observation demonstrates the unique role that SAHCs play in promoting the blue-to-red color transition of the sensor film. Important information on the role played by SAHCs was obtained from an experiment in which a PDA crystal embedded in the PDMS matrix was monitored by using visual microscopy (**Figure 7**). A PDA microcrystal was observed to undergo the blue-to-red color change during the octane initiated swelling process (Figure 7a–d). Interestingly, a significant shrinkage of the crystal takes place when the sensor film is removed from

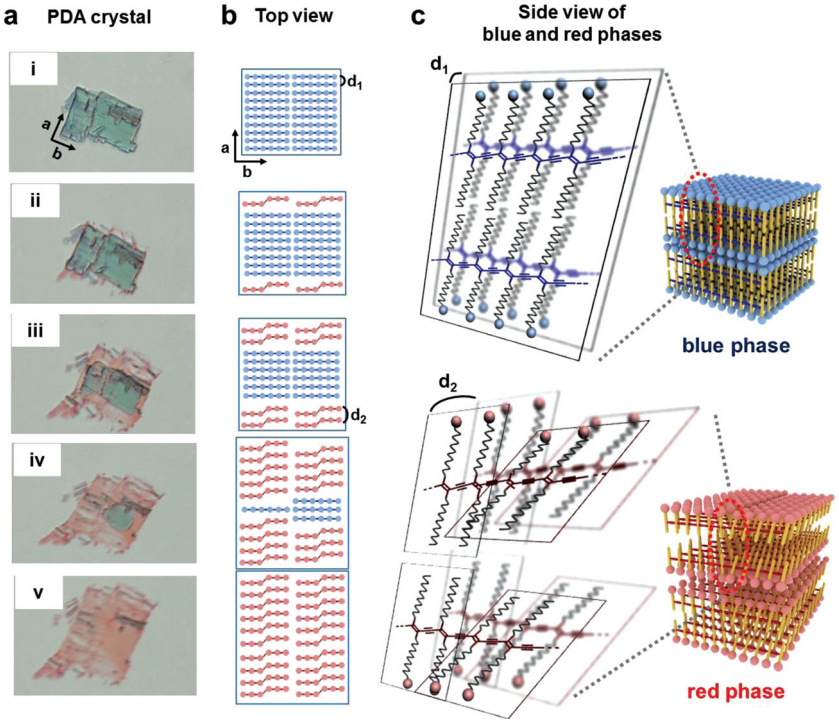

Figure 6. (a) Images showing that a PDA microcrystal experiences drastic color and shape changes during PDMS swelling in octane. It is evident that the blue-to-red color transition is initiated from the edge of the crystal. Microscopic images of the crystal were recorded at 0 (i), 5 (ii), 10 (iii), 15 (iv), 23 (v) min, respectively. (b) Schematic representation of the top-view of a microcrystal during mechanical stretching. The blue and red dots represent each alkyl chain and the phase transition points are shown as diagonal lines. (c) Schematic side views of blue and red phase PDA. An increase in the interchain distance from d_1 to d_2 enables C–C sigma bond rotation that results in twisting of some PDA chains.

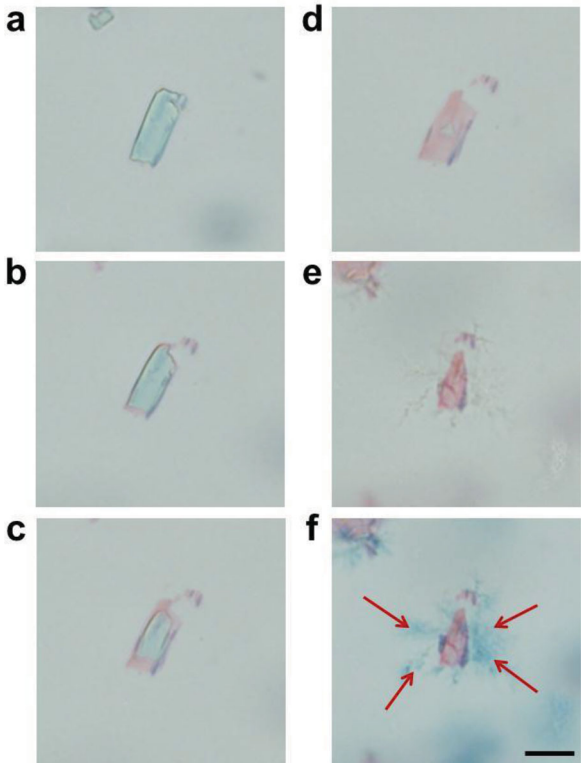

Figure 7. Optical microscopic images of a PDA crystal embedded in a PDMS film recorded at 0 (a), 3 (b), 6 (c), and 9 min (d) after placement in octane. (e) Optical microscopic image of the dried PDA microcrystal from (d). (f) Optical microscopic image of the dried PDA microcrystal after 254 nm UV irradiation (1 mW/cm^2) for 30 s. Appearance of the blue color near the PDA crystal is indicative of the PDA formation. The scale bar is 20 μm.

octane and dried in air (Figure 7e). Surprisingly, UV irradiation (254 nm) of the dried film results in generation of blue colored PDAs near the location of the original PDA microcrystal (Figure 7f, arrow marked areas). This finding strongly suggests that diacetylene monomers are released from the PDA crystal during the PDMS swelling process and that these monomers form self-assembled aggregates upon solvent evaporation, which then participate in UV induced polymerization.

A combination of observations made in this investigation, including the significant increase in the length of the PDA crystal (especially direction perpendicular to the PDA chain) and diacetylene monomer leakage from the polymer crystal during the swelling process, have led to the following proposal. The hydrophobic nature of SAHCs causes the PDA-PDMS film to swell. The large volumetric change occurring during swelling then generates a significant mechanical strain on the PDA supramolecules embedded in the matrix polymer. This perturbation releases unreacted monomers present in the PDA into the hydrocarbon solvent, an event that leads to the creation of voids in the PDA supramolecules, The combined effects of mechanical strain and void creation causes a decrease of interchain interactions in the PDA and serve as a driving force for the PDA phase transition. The above hypothesis was further verified by observing no color change of a PDA-embedded PDMS film derived from hydrocarbon insoluble diacetylene monomer (Supporting Information, Figure S7).

It should be noted that, unlike PDA microcrystals embedded in the PDMS matrix, isolated PDA microcrystals do not undergo swelling or disruption when exposed to octane. Instead, crystal shrinkage and a blue-to-red color transition occur during incubation (Supporting Information, Figure S8). This observation provides further support for the proposal that PDMS swelling is the driving force for disruption of PDA crystals embedded in the polymer matrix.

3. Conclusion

The study described above has led to the development of a new colorimetric hydrocarbon sensor system. The PDA-PDMS composite film constructed in this effort enables visual differentiation of a number of different linear alkanes. Distinction is simply made using blue-to-red colorimetric response times that depend on the chain length of the alkane. The red intensity developed upon incubation of the film in saturated hydrocarbons is directly proportional to the degree of swelling that the film undergoes. The swelling promoted increase in interchain distance between PDA supramolecules within crystals embedded in the film then produces distortion of the arrayed p-orbitals of the conjugated polymer and a simultaneous blue-to-red color transition. A meritorious feature of the sensor system is that it can be employed to detect kerosene in adulterated diesel oils in a simple and convenient manner. Finally, the current investigation has led to the development of a new and potentially general strategy for the colorimetric detection of hydrocarbons. Specifically, it may be possible to design new chromogenic hydrocarbon sensor systems that are based on changes in the absorption and emission properties of functional molecules, which are induced by changes in intermolecular distances associated with volume deformation of a PDMS matrix.

4. Experimental Section

Materials and Instruments: 10,12-Pentacosadiynoic acid (PCDA) was purchased from GFS Chemicals, Ohio, USA. 3-Pentacosa-10,12-diynamidobenzoic acid (PCDA-mBzA) was prepared according to the literature method. Hydrocarbons (C5-C14) were obtained from Aldrich. Polydimethylsiloxane (PDMS, Sylgard 184) was purchased from Dow Corning. Kerosene and diesel oils were purchased from a Hyundai Oil Bank, Korea. Optical microscopic images were collected with a Olympus BX 51W/DP70. Confocal fluorescence microscopic image was obtained with a Olympus IX83/FV1200. UV-visible absorption.

Fabrication of PDA-Embedded PDMS Film: A typical procedure for the preparation of a PDA-embedded PDMS film is as follows. A chloroform solution (0.2 mL), containing commercially available 10,12-pentacosadiynoic acid (PCDA) (2.5 mg), was injected into a PDMS elastomer base (1.0 g). After removing chloroform in vacuo, the mixture was irradiated with a 254 nm UV lamp (1 mWcm^{-2}) for 1 min while stirring. To the resulting, blue colored mixture was added a curing agent (10:1 wt ratio) and the resultant viscous solution was poured into a Petri dish, degassed *in vacuo*, and cured at room temperature for 2 days. This process generated a flexible and transparent PDA-incorporated PDMS film.

Colorimetric Sensing of Hydrocarbons: A blue-colored PDA-embedded PDMS film was placed in a vial containing 4 mL of a specified liquid hydrocarbon. After incubation for 5 min at 25 °C, the sensor strip was

removed from the vial and air dried. The red intensity (RI) values of 10 different spots on the hydrocarbon-treated sample were determined using an Adobe Photoshop program.

Supporting Information

Supporting Information is available from the Wiley Online Library or from the author.

Visible absorption spectra and photographs of PDA embedded polymer films. Confocal and optical microscope images of hydrocarbon treated PDA-embedded PDMS films and PDA microcrystals. Movies showing swelling-induced colorimetric transition of PDA-embedded PDMS films.

Acknowledgements

This work was supported by Nano-Convergence Foundation [Nano-inspired adulterated petroleum detecting sensor system] funded by the Ministry of Science, ICT and Future Planning (MSIP, Korea) & the Ministry of Trade, Industry and Energy (MOTIE, Korea). The authors also thank the National Research Foundation of Korea for financial support through the Basic Science Research Program (2012R1A6A1029029, 2013004800) and Nano-Material Technology Development Program (2012M3A7B4035286).

Received: March 10, 2014
Revised: April 9, 2014
Published online: May 28, 2014

[1] F. Ciardelli, G. Ruggeri, A. Pucci, *Chem. Soc. Rev.* **2013**, *42*, 857.
[2] D. A. Davis, A. Hamilton, J. Yang, L. D. Cremar, D. V. Gough, S. L. Potisek, M. T. Ong, P. V. Braun, T. J. Martinez, S. R. White, J. S. Moore, N. R. Sottos, *Nature* **2009**, *459*, 68.
[3] D. R. T. Roberts, S. J. Holder, *J. Mater. Chem.* **2011**, *21*, 8256.
[4] Y. Chen, A. J. H. Spiering, S. Karthikeyan, G. W. M. Peters, E. W. Meijer, R. P. Sijbesma, *Nat. Chem.* **2012**, *4*, 559.
[5] A. Pucci, G. Ruggeri, *J. Mater. Chem.* **2011**, *21*, 8282.
[6] B. R. Crenshaw, M. Burnworth, D. Khariwala, A. Hiltner, P. T. Mather, R. Simha, C. Weder, *Macromolecules* **2007**, *40*, 2400.
[7] J. R. Kumpfer, S. D. Taylor, W. B. Connick, S. J. Rowan, *J. Mater. Chem.* **2012**, *22*, 14196.
[8] E. P. Chan, J. J. Walish, A. M. Urbas, E. L. Thomas, *Adv. Mater.* **2013**, *25*, 3934.
[9] M. Kolle, A. Lethbridge, M. Kreysing, J. J. Baumberg, J. Aizenberg, P. Vukusic, *Adv. Mater.* **2013**, *25*, 2239.
[10] G. Wegner, *Makromol. Chem.* **1972**, *154*, 35.
[11] R. H. Baughman, R. R. Chance, *J. Polym. Sci. Polym. Phys. Ed.* **1976**, *14*, 2037.
[12] S. R. Diegelmann, J. D. Tovar, *Macromol. Rapid Commun.* **2013**, *34*, 1343.
[13] S. R. Diegelmann, N. Hartman, N. Markovic, J. D. Tovar, *J. Am. Chem. Soc.* **2012**, *134*, 2028.
[14] O. Yarimaga, J. Jaworski, B. Yoon, J.-M. Kim, *Chem. Commun.* **2012**, *48*, 2469.
[15] A. Sun, J. W. Lauher, N. S. Goroff, *Science* **2006**, *312*, 1030.
[16] Y. Lu, Y. Yang, A. Sellinger, M. Lu, J. Huang, H. Fan, R. Haddad, G. Lopez, A. R. Burns, D. Y. Sasaki, J. Shelnutt, C. J. Brinker, *Nature* **2001**, *410*, 913.
[17] S. Rondeau-Gagné, J. R. Néabo, M. Desroches, J. Larouche, J. Brisson, J.-F. Morin, *J. Am. Chem. Soc.* **2013**, *135*, 110.
[18] J. R. Néabo, S. Rondeau-Gagné, C. Vigier-Carrière, J.-F. Morin, *Langmuir* **2013**, *29*, 3446.
[19] A. Deshpande, C.-H. Sham, J. M. P. Alaboson, J. M. Mullin, G. C. Schatz, M. C. Hersam, *J. Am. Chem. Soc.* **2012**, *134*, 16759.
[20] T.-J. Hsu, F. W. Fowler, J. W. Lauher, *J. Am. Chem. Soc.* **2012**, *134*, 142.
[21] Y. Xu, M. D. Smith, M. F. Geer, P. J. Pellechia, J. C. Brown, A. C. Wibowo, L. S. Shimizu, *J. Am. Chem. Soc.* **2010**, *132*, 5334.
[22] D.-C. Lee, S. K. Sahoo, A. L. Cholli, D. J. Sandman, *Macromolecules* **2002**, *35*, 4347.
[23] D. H. Charych, J. O. Nagy, W. Spevak, M. D. Bednarski, *Science* **1993**, *261*, 585.
[24] Q. Xu, S. Lee, Y. Cho, M. H. Kim, J. Bouffard, J. Yoon, *J. Am. Chem. Soc.* **2013**, *135*, 17751.
[25] X. Chen, G. Zhou, X. Peng, J. Yoon, *Chem. Soc. Rev.* **2012**, *41*, 4610.
[26] T. Barisien, J.-L. Fave, S. Hameau, L. Legrand, M. Schott, J. Malinge, G. Clavier, P. Audebert, C. Allain, *ACS Appl. Mater. Interfaces* **2013**, *5*, 10836.
[27] W. Zhang, H. Xu, Y. Chen, S. Cheng, L.-J. Fan, *ACS Appl. Mater. Interfaces* **2013**, *5*, 4603.
[28] E. Gravel, J. Ogier, T. Arnauld, N. Mackiewicz, F. Ducongè, E. Doris, *Chem. Eur. J.* **2012**, *18*, 400.
[29] J. Lee, J. Kim, *Chem. Mater.* **2012**, *24*, 2817.
[30] J. Lee, H.-J. Kim, J. Kim, *J. Am. Chem. Soc.* **2008**, *130*, 5010.
[31] H. Peng, X. Sun, F. Cai, X. Chen, Y. Zhu, G. Liao, D. Chen, Q. Li, Y. Lu, Y. Zhu, Q. Jia, *Nature Nanotechnol.* **2009**, *4*, 738.
[32] X. Chen, L. Li, X. Sun, Y. Liu, B. Luo, C. Wang, Y. Bao, H. Xu, H. Peng, *Angew. Chem. Int. Ed.* **2011**, *50*, 5486.
[33] S. Kolusheva, R. Yossef, A. Kugel, M. Katz, R. Volinsky, M. Welt, U. Hadad, V. Drory, M. Kliger, E. Rubin, A. Porgador, R. Jelinek, *Anal. Chem.* **2012**, *84*, 5925.
[34] I. S. Park, H. J. Park, J.-M. Kim, *ACS Appl. Mater. Interfaces* **2013**, *5*, 8805.
[35] D. Bloor, *Macromol. Chem. Phys.* **2001**, *202*, 1410.
[36] X. Wang, X. Sun, P. A. Hu, J. Zhang, L. Wang, W. Feng, S. Lei, B. Yang, W. Cao, *Adv. Funct. Mater.* **2013**, *23*, 6044.
[37] R. R. Chance, *Macromolecules* **1980**, *13*, 396.
[38] C. Phollookin, S. Wacharasindhu, A. Ajavakom, G. Tumcharern, S. Ampornpun, T. Eaidkong, M. Sukwattanasinitt, *Macromolecules* **2010**, *43*, 7540.
[39] A. Wu, C. Beck, Y. Ying, J. Federici, Z. Iqbal, *J. Phys. Chem. C* **2013**, *117*, 19593.
[40] I. K. Kwon, M. S. Song, S. H. Won, S. P. Choi, M. Kim, S. J. Sim, *Small* **2012**, *8*, 209.
[41] F. Bai, Z. Sun, P. Lu, H. Fan, *J. Mater. Chem.* **2012**, *22*, 14839.
[42] M. P. Leal, M. Assali, I. Fernández, N. Khiar, *Chem. Eur. J.* **2011**, *17*, 1828.
[43] A. Chanakul, N. Traiphol, R. Traiphol, *J. Colloid Interface Sci.* **2013**, *389*, 106.
[44] T. Shimogaki, A. Matsumoto, *Macromolecules* **2011**, *44*, 3323.
[45] S. Ampornpun, S. Montha, G. Tumcharern, V. Vchirawongkwin, M. Sukwattanasinitt, S. Wacharasindhu, *Macromolecules* **2012**, *45*, 9038.
[46] X. Chen, S. Kang, M. J. Kim, J. Kim, Y. S. Kim, H. Kim, B. Chi, S.-J. Kim, J. Y. Lee, J. Yoon, *Angew. Chem. Int. Ed.* **2010**, *49*, 1422.
[47] S. Lee, J. Lee, M. Lee, Y. K. Cho, J. Baek, J. Kim, S. Park, M. H. Kim, R. Chang, J. Yoon, *Adv. Funct. Mater.* **2014**, DOI: 10.1002/adfm.201304147.
[48] R. A. Nallicheri, M. F. Rubner, *Macromolecules* **1991**, *24*, 517.
[49] R. W. Carpick, D. Y. Sasaki, A. R. Burns, *Langmuir* **2000**, *16*, 1270.
[50] H. Feng, J. Lu, J. Li, F. Tsow, E. Forzani, N. Tao, *Adv. Mater.* **2013**, *25*, 1729.
[51] J. N. Lee, C. Park, G. M. Whitesides, *Anal. Chem.* **2003**, *75*, 6544.
[52] M. Florea, W. M. Nau, *Angew. Chem. Int. Ed.* **2011**, *50*, 9338.
[53] N. Bachar, L. Mintz, Y. Zilberman, R. Ionescu, X. Feng, K. Müllen, H. Haick, *ACS Appl. Mater. Interfaces* **2012**, *4*, 4960.

[54] C. S. Rout, A. Govindaraj, C. N. R. Rao, *J. Mater. Chem.* **2006**, *16*, 3936.
[55] I. B. Burgess, N. Koay, K. P. Raymond, M. Kolle, M. Lončar, J. Aizenberg, *ACS Nano* **2012**, *6*, 1427.
[56] W.-E. Lee, C.-L. Lee, T. Sakaguchi, M. Fujiki, G. Kwak, *Macromolecules* **2011**, *44*, 432.
[57] J. Lee, H. T. Chang, H. An, S. Ahn, J. Shim, J.-M. Kim, *Nature Commun.* **2013**, *4*, 2461.
[58] J. Yoon, Y.-S. Jung, J.-M. Kim, *Adv. Funct. Mater.* **2009**, *19*, 209.
[59] J. Yoon, S. K. Chae, J.-M. Kim, *J. Am. Chem. Soc.* **2007**, *129*, 3038.
[60] Fiscal and National Markers, http://www.johnhogg.co.uk/fiscal-markers.html, accessed: December 15, 2013.